

Detecting and Recovering Adversarial Examples: An Input Sensitivity Guided Method

Mingxuan Li
Beihang University
drmeerkatli@gmail.com

Jingyuan Wang
Beihang University
jywang@buaa.edu.cn

Yufan Wu
Beihang University
wuyufan@buaa.edu.cn

Shuchang Zhou
Megvii
zsc@megvii.com

Abstract

*Deep Neural Networks undergo rapid development and have achieved notable successes in various tasks, including many security concerned scenarios. However, a considerable amount of works have proved its vulnerability to adversaries. To address this problem, we propose a **Guided Robust and Efficient Defensive Model (GRED)** integrating detection and recovery processes together. From the lens of the properties of gradient distribution of adversarial examples, our model detects malicious inputs effectively, as well as recovering the ground-truth label with high accuracy. Compared with commonly used adversarial training methods, our model is more efficient and outperforms state-of-the-art adversarial trained models by a large margin up to 99% on MNIST, 89% on CIFAR-10 and 87% on ImageNet subsets. When exclusively compared with previous adversarial detection methods, the detector of GRED is robust under all threat settings with a detection rate of over 95% against most of the attacks. It is also demonstrated by empirical assessment that our model could increase attacking cost significantly resulting in either unacceptable attacking time or human perceptible image distortions.*

1. Introduction

Deep Learning has achieved great success, especially in the field of computer vision. Multiple breakthroughs make it possible to deploy these models into real life applications, including autonomous driving [25], face recognition [34], industrial automation [29] etc.. However, firstly pointed out by Szegedy et al. [41], deep neural networks can be fooled by adding small perturbations to the inputs, which are imperceptible to the human eyes. Since then, lots of work have proved the weakness of deep networks, particularly under computer vision context [1]. These developments draw attention of academia to the security aspect of deep neural networks.

Since then, many defense methods have been proposed,

including robust optimization [26, 15], model architectures modification [6, 13, 36, 42, 38], input reconstruction [17] and some detection based methods [27, 28, 28, 19, 4, 24]. Though making seemingly promising progress against various emerging strong attacks, these methods still have some obstacles to alleviating real world security concerns. These obstacles include requiring large volume of computational resources [26], being unresistant to white-box attacks [7], non-scalable nor tested in bigger datasets and sometimes in need of modifying protected model architectures.

To effectively counteract with these problems, we propose a defensive model called **Guided Robust and Efficient Defensive Model**, namely, **GRED**. This model is inspired by the fact that most of the adversarial attacking algorithms use gradient information of target networks to guide their search for perturbations. The network gradient of adversarial examples may well become the Achilles' heel of attacking algorithms. The GRED model consists of a detection and rectification pipeline. The detection process captures adversarial examples using a gradient-based image sensitivity monitor, and the rectification process recovers true predictions of perturbed images using a gradient-guided rectifier (see Fig. 1). The experiment results over three commonly used datasets show that our model can completely defeat adversaries from several the state-of-the-art attacking algorithms and increase attack cost significantly. Though there are some preliminary works on this topic [12, 43], we exclusively achieve this high performance and show that there are indeed some subtle differences between the norm of gradients of malicious and clean inputs in a more principled way.

The contribution of this paper can be concluded as:

- We find the intrinsic property that can differentiate between adversarial and benign examples guided by the gradient-based input sensitivity of target networks.
- The proposed adversarial example detector achieves a graceful performance (more than 95% detection accuracy) on MNIST, CIFAR-10 and ImageNet under attacks of state-of-the-art algorithms, including DeepFool, CW [9], DDN [35], and PGD [26].

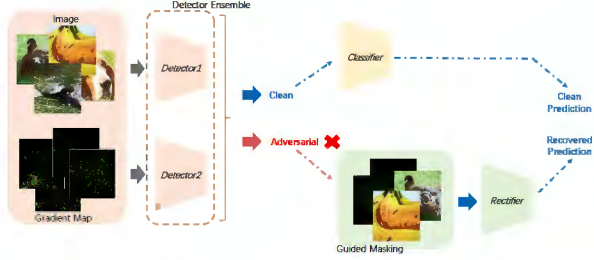


Figure 1. The adversarial examples defense pipeline of GRED.

- To the best of our knowledge, we are the first defense model that achieves such levels of robustness under attack of the DDN scheme, which was the champion of NIPS Adversarial Vision Challenge 2018 schemes and the based model of the challenge 2019.
- Our model also does not require extra modification to the model being protected. This feature is very useful for the neural network system already deployed in the real world.

2. The Basic Idea

In this section, we will briefly introduce our motivation and the inherent idea of our method.

Definition 1 (Classifier) We define a neural network classifier as a function $f: \mathbb{R}^M \rightarrow [0, 1]^L$ with a softmax function as its output.

Definition 2 (Adversarial Sample) For a benign input \mathbf{x} and its predicted label \hat{y} in the classifier f , we define its adversarial counterpart as (\mathbf{x}', \hat{y}') , where $\|\mathbf{x} - \mathbf{x}'\|_2 < \epsilon$ and $\hat{y} \neq \hat{y}'$.

Definition 3 (Input Sensitivity (InSen)) For an input \mathbf{x} and its predicted label \hat{y} , we define its input sensitivity as

$$S(\mathbf{x}, \hat{y}) = \left| \frac{\partial \mathcal{L}(\mathbf{x}, \hat{y})}{\partial \mathbf{x}} \right|, \quad (1)$$

where $\mathcal{L}(\cdot)$ is the cross entropy loss function of f .

Since most of the adversarial attacks use network gradient of input images as a guide to search perturbations [30, 9, 35], the input sensitivity, which is a form of gradient, of a benign sample and its adversarial counterpart usually have significant difference. The basic idea of our method is using InSen as features to design adversarial sample detectors. In order to prove our idea, we give following analysis.

For the sake of discussion, we decompose the classifier f as three parts:

1) The first part is a function that maps an input \mathbf{x} into a representation vector \mathbf{z} , which is denoted as $\mathbf{z} = g(\mathbf{x})$.

2) The second part is a fully connection (FC) layer to calculate the prediction indexes of each classes. For the i -th class, the FC layer calculates an index $a_i = \mathbf{w}_i^\top \cdot \mathbf{z}$.

3) The third part is a softmax function to calculate the prediction probability of each class, which is denoted as $\hat{y} = \sigma(\mathbf{a})$. For class i , this part is in the form of

$$\hat{y}_i = \frac{\exp(a_i)}{\sum_{j=1}^N \exp(a_j)}, i \in \{1, \dots, L\}. \quad (2)$$

In other words, the classifier f is in the form of

$$\hat{y}_i = f_i(\mathbf{x}) = \sigma(\mathbf{w}_i \cdot g(\mathbf{x})), i \in \{1, \dots, L\}. \quad (3)$$

Given two classes m, n , the label of the sample \mathbf{x} with $\mathbf{z} = g(\mathbf{x})$ is decided by the hyperplane as

$$(\mathbf{w}_m - \mathbf{w}_n)^\top \cdot \mathbf{z} > 0. \quad (4)$$

We define a generalized distance of the sample \mathbf{x} to the classification hyperplane as

$$Dist_z(\mathbf{x}) = \frac{|(\mathbf{w}_m - \mathbf{w}_n)^\top \cdot g(\mathbf{x})|}{\|\mathbf{w}_m - \mathbf{w}_n\|_2}. \quad (5)$$

For the sample \mathbf{x} with the predicted class m , its input sensitivity is in the form of

$$S(\mathbf{x}, \hat{y}) = \left| \sum_{p \neq m, n} \frac{C_2}{\sum_q \exp(a_q - a_p)} + \frac{C_1}{\underbrace{\exp((\mathbf{w}_m - \mathbf{w}_n)^\top \mathbf{z})}_{\text{Term I}} + \sum_{q \neq m} \exp(a_q - a_n)} \right|, \quad (6)$$

where $C_1 = \left(\frac{\partial a_n}{\partial \mathbf{x}} - \frac{\partial a_m}{\partial \mathbf{x}} \right)$ and $C_2 = \left(\frac{\partial a_p}{\partial \mathbf{x}} - \frac{\partial a_m}{\partial \mathbf{x}} \right)$. Since the predicted label of \mathbf{x} is m , $a_m > a_n$ and $(\mathbf{w}_m - \mathbf{w}_n)^\top \mathbf{z} > 0$. Therefore, the *Term I* in Eq. (6) is in direct proportion to $Dist_z(\mathbf{x})$. In other words, the InSen $S(\mathbf{x})$ of an example has an increasing trend when its generalized distance to the classification hyperplane decreases, i.e., $Dist_z(\mathbf{x})$ decrease. Therefore, we get following insights:

Insight I: The samples with closer distances to the classification hyperplane usually have larger input sensitivities.

Insight II: For many adversarial attack methods [30, 9, 35], the optimization object restricts size of the perturbations (such as restricting L2 metric of perturbations). Therefore, their adversarial examples are very likely just to cross the decision boundary. Thus, their input sensitivity should be bigger than normal input of that class due to a small $Dist_z$.

Fig. 2 illustrates the L_2 norms of InSen for clean and malicious inputs from MNIST and CIFAR-10 (setups see the experiment section). The InSen size of clean data are very tiny, while that of the malicious data are quite gigantic. This empirical result confirmed our Insights. We can use the InSen as a feature to detect adversarial samples.

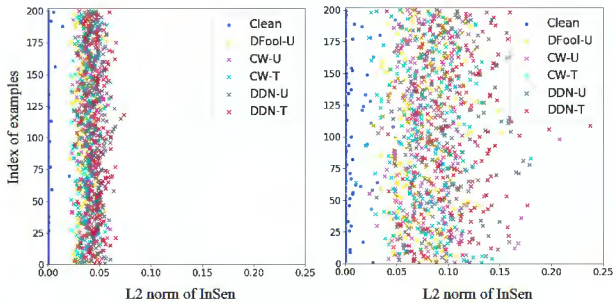


Figure 2. L_2 norm of InSen for clean and adversarial examples. Left: MNIST; Right: CIFAR-10.

3. Framework

In this section, we introduce each component and full processing pipeline of the **Guided Robust and Efficient Defensive** model (GRED). The GRED model consists of two components: a detector to distinguish adversarial examples from benign examples, and a rectifier to recover adversarial examples back to benign ones.

3.1. Adversarial Example Detector

Given a set of benign examples $X = \{\mathbf{x}_1, \dots, \mathbf{x}_N\}$, a classifier to be protected, denoted as $f: \mathbb{R}^M \rightarrow [0, 1]^L$, and an adversarial attack method, we can generate a set of adversarial counterparts of X as $X' = \{\mathbf{x}'_1, \dots, \mathbf{x}'_N\}$. Combining X and X' , we got a data set in the form of

$$\mathcal{X} = \{(\mathbf{x}_1, \mathbf{l}_1), \dots, (\mathbf{x}_N, \mathbf{l}_N), (\mathbf{x}'_1, \mathbf{l}'_1), \dots, (\mathbf{x}'_N, \mathbf{l}'_N)\}, \quad (7)$$

where $\mathbf{l} = (l^+, l^-)$ is a one-hot coding of benign/adversarial label. $\mathbf{l}_n = (1, 0)$ for benign examples and $\mathbf{l}'_n = (0, 1)$ for adversarial examples.

The GRED model uses the data set \mathcal{X} to train two classifiers. The first classifier adopts \mathbf{x}_n (or \mathbf{x}'_n) as inputs of a convolutional neural network (CNN) to predict their benign/adversarial labels, *i.e.*,

$$(p^+, p^-) = CNN_{org}(\mathbf{x}), \quad (8)$$

where $p^+ \in [0, 1]$ is the probability of the input being benign, $p^- \in [0, 1]$ is the probability of being adversarial ones, and $p^+ + p^- = 1$. A similar classifier as (8) is also adopted by Gong *et al.* [14] to detect adversarial examples.

However, as reported by Carlini and Wagner [7], only using original image feature \mathbf{x} is not enough for advance adversarial attack method defense. Therefore, GRED introduces the other classifier which uses $S(\mathbf{x})$ as inputs of a CNN network to predict benign/adversarial labels, *i.e.*,

$$(p^+, p^-) = CNN_{sen}(S(\mathbf{x}, \hat{\mathbf{y}})), \quad (9)$$

Removed High InSen Pixels	Attack Success Rate		
	Deepfool	CW	DDN
top 0%	1.000	1.000	1.000
top 5%	0.637	0.665	0.656
top 10%	0.780	0.794	0.785

Table 1. Attack success rates of adversarial examples without top 5% and 10% high InSen pixels.

where $S(\mathbf{x}, \hat{\mathbf{y}})$ is the input sensitivity of sample \mathbf{x} , which is calculated using Eq. (1). The image label $\hat{\mathbf{y}}$ is generated by the classifier to be protected.

Both of the classifiers in Eq. (8) and Eq. (9) are optimized using a cross entropy loss function as

$$\mathcal{L}_{cnn} = - \sum_{n=1}^N (l_n^+ \log p_n^+ + l_n^- \log p_n^-). \quad (10)$$

Given an input, we denote the outputs of CNN_{org} and CNN_{sen} as $p_o = (p_o^+, p_o^-)$ and $p_s = (p_s^+, p_s^-)$, respectively. For the two predicted labels, GRED estimates the information entropy they could offer as

$$\begin{aligned} H_o &= - [p_o^+ \log_2(p_o^+) + p_o^- \log_2(p_o^-)], \\ H_s &= - [p_s^+ \log_2(p_s^+) + p_s^- \log_2(p_s^-)]. \end{aligned} \quad (11)$$

The prediction from the classifier that is more confident is adopted as the final prediction of GRED, *i.e.*,

$$(p^+, p^-) = \begin{cases} p_o & \text{if } H_o < H_s \\ p_s & \text{if } H_o \geq H_s \end{cases}. \quad (12)$$

The GRED model considers the images with $p^+ \geq p^-$ as benign examples, of which the labels of the original image classification task are directly given by the classifier f . On the contrary, the images with $p^+ < p^-$ are considered as adversarial examples. Their image classification label should be further recovered by a rectifier.

3.2. Adversarial Example Rectifier

The design of the rectifier is inspired by the following insight:

Insight III: As mentioned in Sec. 2, the L_2 norms of input sensitivity for adversarial examples are significant larger than benign examples. Thus, the pixels with large input sensitivity $|\partial \mathcal{L} / \partial x_i|$ are very likely to have been modified by the attack algorithm. Therefore, we conjecture if we remove the polluted pixels guided by their InSen, the attack effects of adversarial examples might be dampened.

Table 1 are results of an experiment for verification. In the experiment, we use three methods, Deepfool [30], CW [9] and DDN [35], to generate adversarial examples for a VGG11 network, and set the pixels with top 5% and 10%

biggest $|\partial\mathcal{L}/\partial x_i|$ as zero respectively. As shown in the table, when we use original adversarial examples to attack the VGG11 network, the success rate is 100%, but when we use adversarial examples without top 5% high InSen pixels to attack, the success rate falls to only 63.7%. This experiment results confirmed our conjecture that high InSen could be used as indexes to pick polluted pixels out from an adversarial example. When the ratio of removed pixels increases, the success rate increases again. The reason is too many zero pixels may reduce the accuracy of the classifier. This requires us to design an elaborate approach to pick out the polluted pixels. Based on the phenomenon revealed by Tab. 1, we proposed our rectifier model.

We define an adversarial example that is detected by the detector as a matrix \mathbf{X} , where the element $x_{a,b}$ is the pixel at the location (a,b) ¹. We select a pixel as a suspect when its InSen larger than a threshold as

$$\left| \frac{\partial\mathcal{L}}{\partial x_{a,b}} \right| > \alpha \cdot (S_{max} - S_{min}) + S_{min}, \quad (13)$$

where S_{max} and S_{min} are the maximum and minimum values of pixel’s InSen in the image \mathbf{X} , and α is a preset parameter to control the ratio of suspect pixels.

For a suspect pixel, GRED randomly disables it using two random numbers x_{ran} and u_{ran} as

$$x_{a,b} := \begin{cases} x_{a,b} & \text{if } u_{ran} = 0 \\ x_{ran} & \text{if } u_{ran} = 1 \end{cases}, \quad (14)$$

where $u_{ran} \in \{0,1\}$ follows a Bernoulli distribution. If $u_{ran} = 0$, we keep $x_{a,b}$ as its raw value, otherwise we set it as a random value $x_{ran} \in [0,255], x_{ran} \in \mathbb{N}$. x_{ran} follows a normal distribution $N(\sigma, \mu)$, where σ, μ are set as the mean and standard deviation of pixels in \mathbf{X} .

In this way, we can generate many randomized duplicates for every adversarial example \mathbf{X}_i . We collect these randomized duplicates as a data set \mathcal{X}_{ran} , and use \mathcal{X}_{ran} to fine tune the original image classifier f as the rectifier f_{rec} .

Compared with the original image classifier f , the rectifier f_{rec} is more robust to adversarial examples. However, its performance for benign examples is a little worse than f due to some image information in \mathcal{X}_{ran} were erased by the randomization. In order to combine the advantages of both f and f_{rec} . We only use the rectifier to classify the adversarial examples picked out by the detector, and still handle benign examples with the original classifier.

4. Experiment

4.1. Dataset

In the experiments, we test our model with three popular image datasets. All the pixels are scaled to fall in $[0,1]$.

¹For the sake of discussion, we use the signal channel image as an example to introduce our rectifier.

1) MNIST [23] contains 70,000 greyscale images of handwritten digits from 0 to 9. In the dataset, 60,000 images are for training and 10,000 for testing. The image size is 28×28 .

2) CIFAR-10 [20] contains 60,000 color images corresponding to 10 different object classes. In the dataset, 10,000 images are for training and 50,000 for testing. The image size is 32×32 .

3) ImageNet [11] is a large natural image dataset containing over 1.2 million images. We select images of 20 object classes from the dataset for our experiment. Each class contains 1,040 training samples and 260 test samples. All these images are resized to 256×256 and center cropped to 224×224 .

4.2. Adversarial Examples Generation

We use VGG11 [37] as base classifier on the MNIST and CIFAR-10 datasets. Our base classifiers obtain test accuracy of 99.17% and 84.41% on MNIST and CIFAR-10 respectively. For our ImageNet subset, we use a pre-trained ResNet152 [18] with 95.25% prediction accuracy on the test set.

Experiments are conducted on five extensively used and state of the art attacks, which are FGSM [15], Deepfool (DFool) [30], PGD [26], CW [9] and DDN [35]. For each algorithm, we evaluate our model on two types of threats, *i.e.*, untargeted and targeted [1].

1) *Untargeted Attack*: For a classifier $f: \mathbb{R}^M \rightarrow [0,1]^L$ equipped with a detector, an input image can be classified into $L+1$ classes, *i.e.*, L object classes and one adversarial class y_{adv} . For an image with an original prediction of \hat{y}_{true} , its untargeted adversarial counterpart is successful only when the perturbed predicted label \hat{y}' satisfies $\hat{y}' \neq \hat{y}_{true}$ and $\hat{y}' \neq y_{adv}$.

2) *Targeted Attack*: For an image with an original predicted label \hat{y}_{true} , its targeted adversarial counterpart is successful only when the perturbed label \hat{y}' satisfies $\hat{y}' = y_{target}, y_{target} \neq \hat{y}_{true}$. In our experiments, the given target label y_{target} is chosen randomly.

In the experiments, we mark the untargeted version of attack algorithms with the postfix “-U”, and the targeted attack version with “-T”. FGSM and Deepfool only have untargeted version, while PGD, CW, DDN have both targeted and untargeted versions.

Then we evaluate our model under three attack scenarios: black-box, white-box, and grey-box.

1) *Black-box Attack*: The attacker has no access to the classifier model and does not know if the model is under protection.

2) *Grey-box Attack*: The attacker has knowledge of the network parameters and structures of the target model but is not aware that the target model is under the protection of some defensive mechanism.

MNIST					
Attacker	Attack Rate	Detector Prediction Accuracy			
		DET_{org}	DET_{sal}	DET_{IS}	DET_{GRED}
FGSM-U	0.351	1.000	1.000	0.928	1.000
PGD-U	1.000	1.000	1.000	0.513	1.000
PGD-T	1.000	1.000	1.000	0.505	0.999
DFool-U	1.000	0.991	0.994	0.995	0.998
CW-U	1.000	0.988	0.994	0.996	0.996
CW-T	1.000	0.996	0.996	0.996	0.999
DDN-U	1.000	0.992	0.995	0.997	0.998
DDN-T	1.000	0.998	0.998	0.997	0.999

CIFAR10					
Attacker	Attack Rate	Detector Prediction Accuracy			
		DET_{org}	DET_{sal}	DET_{IS}	DET_{GRED}
FGSM-U	0.806	1.000	1.000	0.732	1.000
PGD-U	0.898	0.998	0.998	0.505	0.998
PGD-T	0.819	0.998	0.997	0.519	0.994
DFool-U	1.000	0.503	0.505	0.954	0.954
CW-U	1.000	0.503	0.503	0.958	0.958
CW-T	0.999	0.512	0.512	0.950	0.950
DDN-U	1.000	0.505	0.504	0.966	0.966
DDN-T	1.000	0.511	0.518	0.966	0.966

ImageNet					
Attacker	Attack Rate	Detector Prediction Accuracy			
		DET_{org}	DET_{sal}	DET_{IS}	DET_{GRED}
FGSM-U	0.732	0.992	0.992	0.897	0.957
PGD-U	0.997	0.998	0.999	0.501	0.998
PGD-T	0.990	0.998	0.998	0.550	0.997
DFool-U	0.993	0.502	0.503	0.976	0.976
CW-U	0.999	0.502	0.502	0.943	0.943
CW-T	0.997	0.501	0.503	0.953	0.952
DDN-U	1.000	0.502	0.502	0.979	0.979
DDN-T	1.000	0.502	0.502	0.986	0.986

Win Count	8	8	11	19
-----------	---	---	----	----

Table 2. Summary of the adversary success rate and detector prediction performance for grey-box scenario. Attack Rate stands for adversary success rate.

3) *White-box Attack*: The attacker is aware that the target model is under the protection of a specific defense, and has full access to the target model and the defensive scheme.

4.3. Performance of Detector

In this section we evaluate our detector in different attack scenarios. All the detectors use a VGG11 unless specified. Here, we compare the proposed detector DET_{GRED} with three baselines:

1) DET_{org} uses original image as input to train a detector [14] (see Eq. (8)).

2) DET_{sal} uses saliency maps of network middle layers as features to train a detector, which is first proposed by Zhang *et al.* [43].

3) DET_{IS} only uses input sensitivity to train a detector (see Eq. (9)).

Performances of the detectors are listed in Tab. 2.

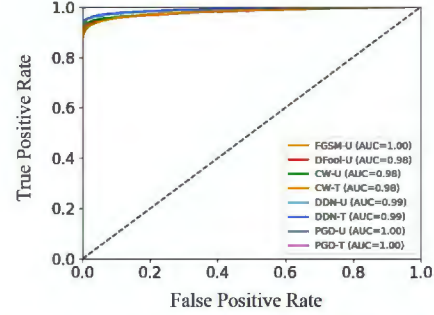


Figure 3. ROC curve of our detector against different attacks under grey-box threat.

MNIST					
Attacker	Attack Rate	Detector Prediction Accuracy			
		DET_{org}	DET_{sal}	DET_{IS}	$GRED$
FGSM-U	0.173	1.000	1.000	0.773	0.977
PGD-U	0.114	1.000	1.000	0.707	0.966
PGD-T	0.433	1.000	1.000	0.700	0.945
DFool-U	1.000	0.994	0.994	0.797	0.994
CW-U	1.000	0.988	0.982	0.974	0.998
CW-T	0.882	0.971	0.971	0.777	0.967
DDN-U	1.000	0.994	0.986	0.976	0.998
DDN-T	1.000	0.996	0.998	0.892	0.996

CIFAR10					
Attacker	Attack Rate	Detector Prediction Accuracy			
		DET_{org}	DET_{sal}	DET_{IS}	$GRED$
FGSM-U	0.941	0.998	1.000	0.514	0.990
PGD-U	0.114	1.000	1.000	0.707	0.966
PGD-T	0.433	1.000	1.000	0.700	0.945
DFool-U	1.000	0.502	0.500	0.930	0.930
CW-U	1.000	0.493	0.491	0.941	0.941
CW-T	1.000	0.505	0.514	0.932	0.934
DDN-U	1.000	0.507	0.495	0.945	0.945
DDN-T	1.000	0.511	0.507	0.952	0.952

ImageNet					
Attacker	Attack Rate	Detector Prediction Accuracy			
		DET_{org}	DET_{sal}	DET_{IS}	DET_{GRED}
FGSM-U	0.603	0.996	0.991	0.500	0.965
PGD-U	0.114	1.000	1.000	0.707	0.966
PGD-T	0.433	1.000	1.000	0.700	0.945
DFool-U	0.979	0.503	0.500	0.946	0.946
CW-U	1.000	0.503	0.497	0.929	0.929
CW-T	1.000	0.503	0.500	0.934	0.931
DDN-U	0.979	0.503	0.495	0.946	0.946
DDN-T	1.000	0.497	0.500	0.939	0.939

Win Count	8	9	14	18
-----------	---	---	----	----

Table 3. Summary of the adversary success rate and detector prediction performance for black-box scenario. Attack Rate stands for adversary success rate.

4.3.1 The Grey-box Attacks

For grey-box attacks, the attacker has full access to base classifiers' structures and parameters, but the attacker does not know the existence of our detector. According to the definition of grey-box attacks mentioned above, adversarial examples are not optimized for the detector. This is a

favorable condition for our detector, since the enemies are exposed, but we are in a shelter. Firstly, we evaluate detection performance of our model in a grey-box scenario.

Tab. 2 shows results of grey-box attacks. As shown in the table, we observe that:

1) The DET_{GRED} achieves above 95% accuracy for all datasets and all attacks, which indicates our model’s high effectiveness. ROC results are listed in Fig. 3.

2) The DET_{org} and DET_{sal} perform well on MNIST, but they perform poorly on CIFAR-10 and ImageNet. This result indicates that it is not suitable to use original images or saliency maps solely as features to detect adversarial examples is not suitable for natural images.

3) DET_{IS} has good performance for all of the three datasets, which verifies the Insight I we proposed in Sec. 2.

4) For FGSM and PGD attacks, the performance of DET_{org} is better than DET_{IS} . As we would analyze later in the black-box scenario, the input sensitivities of adversarial examples from these two attacks are not as high as other attacks. The reason lies behind is they are not bounded by L_2 norm, while they are easily detected by DET_{org} as the pixel space distortion is big enough.

5) DET_{GRED} benefits from both DET_{IS} and DET_{org} using Eq. (12) and achieves the best average performance (estimated by Win Count), which is close to the better one between DET_{IS} and DET_{org} for most of the time.

4.3.2 The Black-box Attacks

In real world applications, it is hardly possible for attackers to have full access to classification models. Due to the transferability of adversary, attacker can still generate adversarial examples on an open-source model to launch the attack. Therefore, we simulate this situation by evaluating our detector in the black-box attack scenario. Black-box attacks is harder than grey-box, because our detector is not directly optimized for the adversarial examples generated by the attacker. In other words, we are in a shelter and enemies are partly in a shelter too.

In the experiment, we transfer adversarial examples from a trained CWnet [9] for MNIST and CIFAR-10 with 99.08% and 84.13% accuracy respectively. For ImageNet, we use a pre-trained InceptionV3 [40] with 94.58% accuracy (on our ImageNet subset). The experiment results are listed in Tab. 3. The result shows that,

1) The performance of DET_{GRED} is at least 92% under all conditions. In particular, we successfully defeat DDN [35], which ranks first in untargeted track and third in targeted track of NIPS 2018 Adversarial Visual Challenge [5].

2) The performance of DET_{IS} decreases for FGSM and PGD. But the attack success rates also decrease drastically. Therefore, they are not substantial threats to our defense method.

According to our Insight II, DET_{IS} is sensitive to L_2 bounded attackers while FGSM and PGD are L_∞ bounded. Thus, they have relatively larger perturbations and smaller input sensitivities which is more closer to that of clean images.

To further verify our hypothesis, we calculate the L_2 norm of InSen for adversarial examples from FGSM and PGD. From the statistics, it is proved that their InSen is quite similar with that of benign examples. Exactly opposite to what is shown in Fig. 2, the InSen of L_2 bounded adversarial examples is significantly higher than that of benign examples.

4.3.3 The White-box Attacks

In this scenario, attackers have full knowledge of our defensive model and they can generate adversarial examples accordingly. We evaluate our model under targeted and untargeted attacks. For targeted attacks, we use the method proposed by Carlini&Wagner [7], which treats our GRED model as a $L + 1$ classifier, *i.e.*, L natural classes and an adversarial class. For the untargeted attacks, we adopt a two-stage scheme to search for perturbations. See details in supplementary.

As suggested by Carlini and Wagner [7], a successful white-box attack should not be detected by the detector as well as fooling the classifier. The adversarial examples that cannot bypass the detector or fail to fool the classifier are not successful.

Therefore, we use success rate of adversarial examples to evaluate performance of our detectors. We consider an attacker fails when its attack success rates is less than 50%. From Tab. 5 and Tab. 4, we can see that,

1) Our model GRED can successfully defeat FGSM, PGD, and CW.

2) Our model achieves full success on ImageNet subset. The defense fails when it is tested against the untargeted Deepfool on CIFAR-10, untargeted DDN on MNIST and targeted DDN on CIFAR-10. We highlighted these failed defenses with blue in the table.

However, does this defense really fail? We need to open the box to look into some details. Tab. 6 given the L_2 perturbations of these three “failed” cases. As shown in the table, for the untargeted case, there are some examples which can bypass our defense, but it is at the cost of increasing the mean L_2 perturbation 40% or even 1200%. Fig. 4 gives example perturbed images. The noise can be observed by human easily! Therefore, we cannot say these samples are “successful”.

Besides, for the targeted DDN case, of which the L_2 perturbations is very small, we still cannot say the attack is “success” due to huge computing resource consumption. In our experiments, it spends about 40 hours to train the tar-

Attacker	MNIST			CIFAR10			ImageNet		
	NoDET	DET_{IS}	DET_{GRED}	NoDET	DET_{IS}	DET_{GRED}	NoDET	DET_{IS}	DET_{GRED}
FGSM	0.271	0.012	0.000	0.315	0.009	0.000	0.608	0.566	0.180
DFool	1.000	0.828	0.286	1.000	0.738	0.734	0.995	0.087	0.087
PGD	1.000	0.871	0.263	0.945	0.805	0.143	1.000	0.359	0.425
CW	1.000	0.000	0.008	1.000	0.009	0.023	1.000	0.009	0.023
DDN	1.000	0.004	0.941	1.000	0.019	0.014	1.000	0.159	0.092

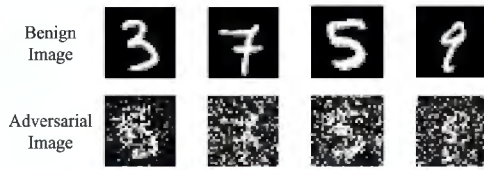
Table 4. Attack success rate under untargeted white-box attacks. Smaller is better.

Attacker	MNIST			CIFAR10			ImageNet		
	NoDET	DET_{IS}	DET_{GRED}	NoDET	DET_{IS}	DET_{GRED}	NoDET	DET_{IS}	DET_{GRED}
PGD	1.000	1.000	0.437	0.957	0.734	0.463	1.000	0.456	0.485
CW	1.000	0.180	0.471	1.000	0.556	0.321	0.995	0.056	0.015
DDN	1.000	0.808	0.392	1.000	1.000	1.000	1.000	0.338	0.326

Table 5. Attack success rate under targeted white-box attacks. Smaller is better.

Attacker	DDN-U	Dfool-U	DDN-T
Without detector	0.787	0.291	0.45
With DET_{GRED}	10.252	0.652	0.618

Table 6. The L2 perturbations of the three “fail” defenses



(a) Untargeted DDN for MNIST



(b) Untargeted Deepfool for CIFAR-10

Figure 4. Example perturbed images of “fail” defenses.

ged DDN attacker over 10,000 CIFAR10 dataset. However, if we train the same attacker to the classifier without detector over the same dataset, it only spent one hour. We believe the time consumption becomes unacceptable for training an attacker that can fool a classifier protected by our detector when it comes to a huge real-world image dataset.

4.4. Performance of Rectifier

Next, we test the performance of the rectifier. The implementation of the rectifier includes two steps: 1) generating images with InSen guided random mask; 2) using the masked images to fine tune classifier. Both two steps contribute performance improvement to the rectifier. Therefore, we conduct analysis on these two steps respectively.

We first evaluate how different masking rate influences the performance of InSen guided rectification. Fig. 5 shows

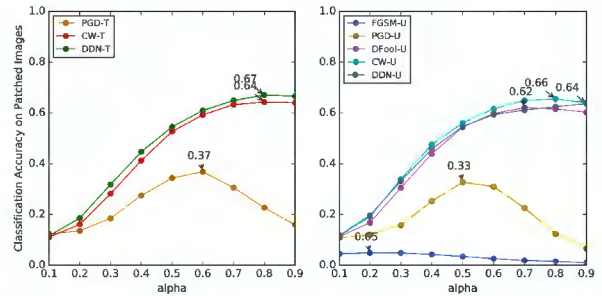


Figure 5. Influence of different masking rate on the rectifier’s performance. Left: Targeted. Right: Untargeted.

the rectifier performance on adversarial examples of our ImageNet subset. We vary the parameter α , which controls the masking rate, in Eq. (13) from 10% to 90%. Obviously, neither too large nor too small α is a good choice. Too small α cannot eliminate the influence of adversarial perturbations; too large α may cause loss of too much image information. As shown in Fig. 5, a reasonable masking rate is around 0.3 – 0.6 depending on attack methods. The classification accuracy can reach more than 80% under the grey-box condition.

Secondly, we use previously found optimal α value to mask adversarial examples and uses the masked examples to fine tune the base classifier as a rectifier. The first part of Tab. 7 lists the adversarial example classification performance of the rectifiers for different datasets under grey-box condition. As shown by the table, the recovery performance for the adversarial examples can reach over 85% in most cases. This defense performance is superior to state-of-the-art adversarial trained models including Madry Defense [26] and DDN [35]. The recovering performance in black-box and white-box conditions are similar. We do not list them due to the space limitation.

All Examples are Adversarial									
	Classifier Acc	FGSM-U	PGD-U	PGD-T	DFool-U	CW-U	CW-T	DDN-U	DDN-T
MNIST	0.000	0.987	0.973	0.967	0.994	0.992	0.994	0.993	0.992
CIFAR10	0.000	0.864	0.898	0.860	0.868	0.879	0.860	0.881	0.872
ImageNet	0.000	0.702	0.810	0.807	0.868	0.837	0.768	0.870	0.844
Adversarial and Benign Examples Mixed									
	Classifier Acc	FGSM-U	PGD-U	PGD-T	DFool-U	CW-U	CW-T	DDN-U	DDN-T
MNIST	0.500	0.994	0.990	0.983	0.997	0.995	0.997	0.996	0.996
CIFAR10	0.500	0.933	0.949	0.930	0.943	0.946	0.934	0.948	0.949
ImageNet	0.500	0.826	0.904	0.904	0.926	0.902	0.882	0.930	0.918

Table 7. Classification Accuracy of the GRED model. Top: Recrifier performance. Below: End-to-end performance.

4.5. Performance of joint defense

Finally, we estimate the end-to-end performance of the GRED model by combining the detector and the rectifier into a pipeline. Full model architecture is in Fig. 1.

In real world applications, adversarial and benign examples are mixed. Therefore, we build datasets where adversarial and benign examples are in equal proportions. The second part of Tab. 7 records the performance of joint defense in this condition (grey-box attacks). The original classification performance for benign examples over these datasets are also listed for your reference. We can see that the defense performance of the GRED model can easily reach over 90% accuracy on end-to-end mixed classification task. This result verifies the effectiveness of our GRED model for end-to-end adversarial examples defense.

It is worthy of mention that,

1) Here we train our PGD detectors using the same parameters reported in [26] on MNIST and CIFAR-10. Their adversarial trained Wide ResNet/simple ResNet can only achieve around 45% accuracy on CIFAR-10, while our VGG11 classifier could achieve more than 80%. The situation is same for MNIST. This also dampens their claim on the influence of model capacity to the robustness.

2) Our VGG11 achieves 99% and 88% on MNIST and CIFAR-10 respectively, while adversarial trained InceptionV3 using DDN [35] only achieves 87% and 67%.

5. Related Work

Previous research on finding adversarial examples assume attackers have full access to the models called “white box” attacks. Many widely applied attacks leverage gradient of the model to guide their search towards efficient perturbations [9, 21, 15, 39, 30, 35, 26]. In a more realistic setting, direct access to the target model is not always available to attackers. Thus, subsequent work also focuses on “black box” attacks [31, 32, 2, 16]. From an optimization perspective, to search for a suitable adversarial perturbation is to solve a certain object function with constrained noise payload under some measures like L_0, L_2, L_∞ .

The methods proposed to mitigate the threats of adver-

saries could mainly be divided into two categories. One is to make robust predictions against adversaries directly. This could be done in various approaches including robust optimization, model architecture modification and inference time reconstruction of inputs. 1) Robust optimization [26, 15] mainly augments the training data by adding adversarial examples to train a robust classifier. It usually requires online update of training data consuming exorbitant time and computational resources which makes it difficult at ImageNet scale [22]. 2) Modifying model architectures [6, 13, 36, 42, 38] typically means manipulating the model gradients to make it intractable at inference time for adversarial attacks or use sub networks like defensive distillation [33]. These methods have also been proved to be ineffective [3, 10]. 3) Reconstruction of inputs [17] during inference time could remove input perturbations to some extent so that the input could be classified correctly. This method could also be bypassed with BPDA [3] which approximates the gradient of the target network.

Considering the hardness of counteracting attacks directly, another main stream of method focuses on the detection of adversarial examples. Approaches include using auxiliary neural networks [27, 28] to decide if input is clean or adversarial, using statistical methods to verify properties of the image or the network parameters [28, 19, 4, 24]. However, Carlini and Wagner proved that under calibrated attacks these methods are still ineffective [7, 8].

6. Conclusion

In this paper, we reveal that one intrinsic property, the Input Sensitivity, can differentiate adversarial examples from clean images and proposed a adversarial attacking defense model named as GRED based on the property. Our model is more efficient and outperforms state-of-the-art adversarial trained models by a large margin: up to 99% on MNIST, 89% on CIFAR-10 and 87% on ImageNet subsets. To the best of our knowledge, we are the first to achieve these levels of robustness under attacks of SOTA methods like DDN.

References

- [1] Naveed Akhtar and Ajmal Mian. Threat of adversarial attacks on deep learning in computer vision: A survey. *IEEE Access*, 6:14410–14430, 2018. 1, 4
- [2] Moustafa Alzantot, Yash Sharma, Supriyo Chakraborty, Huan Zhang, Cho-Jui Hsieh, and Mani B Srivastava. GenAttack: Practical black-box attacks with gradient-free optimization. In *Proceedings of the Genetic and Evolutionary Computation Conference*, pages 1111–1119. ACM, 2019. 8
- [3] Anish Athalye, Nicholas Carlini, and David A. Wagner. Obfuscated gradients give a false sense of security: Circumventing defenses to adversarial examples. In *Proceedings of the 35th International Conference on Machine Learning, ICML 2018, Stockholm, Sweden, July 10-15, 2018*, pages 274–283, 2018. 8
- [4] Arjun Nitin Bhagoji, Daniel Cullina, and Prateek Mittal. Dimensionality reduction as a defense against evasion attacks on machine learning classifiers. *CoRR*, abs/1704.02654, 2017. 1, 8
- [5] Wieland Brendel, Jonas Rauber, Alexey Kurakin, Nicolas Papernot, Behar Veliqi, Marcel Salathé, Sharada Prasanna Mohanty, and Matthias Bethge. Adversarial vision challenge. *CoRR*, abs/1808.01976, 2018. 6
- [6] Jacob Buckman, Aurko Roy, Colin Raffel, and Ian J. Goodfellow. Thermometer encoding: One hot way to resist adversarial examples. In *6th International Conference on Learning Representations, ICLR 2018, Vancouver, BC, Canada, April 30 - May 3, 2018, Conference Track Proceedings*, 2018. 1, 8
- [7] Nicholas Carlini and David Wagner. Adversarial examples are not easily detected: Bypassing ten detection methods. In *Proceedings of the 10th ACM Workshop on Artificial Intelligence and Security*, pages 3–14. ACM, 2017. 1, 3, 6, 8
- [8] Nicholas Carlini and David Wagner. Magnet and” efficient defenses against adversarial attacks” are not robust to adversarial examples. *arXiv preprint arXiv:1711.08478*, 2017. 8
- [9] Nicholas Carlini and David Wagner. Towards evaluating the robustness of neural networks. In *2017 IEEE Symposium on Security and Privacy (SP)*, pages 39–57. IEEE, 2017. 1, 2, 3, 4, 6, 8
- [10] Nicholas Carlini and David A. Wagner. Defensive distillation is not robust to adversarial examples. *CoRR*, abs/1607.04311, 2016. 8
- [11] J. Deng, W. Dong, R. Socher, L.-J. Li, K. Li, and L. Fei-Fei. ImageNet: A Large-Scale Hierarchical Image Database. In *CVPR09*, 2009. 4
- [12] Jasjeet Dhaliwal and Saurabh Shintre. Gradient similarity: An explainable approach to detect adversarial attacks against deep learning. *arXiv preprint arXiv:1806.10707*, 2018. 1
- [13] Guneet S. Dhillon, Kamyar Azizzadenesheli, Zachary C. Lipton, Jeremy Bernstein, Jean Kossaifi, Aran Khanna, and Animashree Anandkumar. Stochastic activation pruning for robust adversarial defense. In *6th International Conference on Learning Representations, ICLR 2018, Vancouver, BC, Canada, April 30 - May 3, 2018, Conference Track Proceedings*, 2018. 1, 8
- [14] Zhitao Gong, Wenlu Wang, and Wei-Shinn Ku. Adversarial and clean data are not twins. *CoRR*, abs/1704.04960, 2017. 3, 5
- [15] Ian Goodfellow, Jonathon Shlens, and Christian Szegedy. Explaining and harnessing adversarial examples. In *International Conference on Learning Representations*, 2015. 1, 4, 8
- [16] Chuan Guo, Jacob Gardner, Yurong You, Andrew Gordon Wilson, and Kilian Weinberger. Simple black-box adversarial attacks. In Kamalika Chaudhuri and Ruslan Salakhutdinov, editors, *Proceedings of the 36th International Conference on Machine Learning*, volume 97 of *Proceedings of Machine Learning Research*, pages 2484–2493, Long Beach, California, USA, 09–15 Jun 2019. PMLR. 8
- [17] Chuan Guo, Mayank Rana, Moustapha Cissé, and Laurens van der Maaten. Countering adversarial images using input transformations. In *6th International Conference on Learning Representations, ICLR 2018, Vancouver, BC, Canada, April 30 - May 3, 2018, Conference Track Proceedings*, 2018. 1, 8
- [18] Kaiming He, Xiangyu Zhang, Shaoqing Ren, and Jian Sun. Deep residual learning for image recognition. In *2016 IEEE Conference on Computer Vision and Pattern Recognition, CVPR 2016, Las Vegas, NV, USA, June 27-30, 2016*, pages 770–778, 2016. 4
- [19] Dan Hendrycks and Kevin Gimpel. Early methods for detecting adversarial images. In *5th International Conference on Learning Representations, ICLR 2017, Toulon, France, April 24-26, 2017, Workshop Track Proceedings*, 2017. 1, 8
- [20] Alex Krizhevsky et al. Learning multiple layers of features from tiny images. Technical report, Citeseer, 2009. 4
- [21] Alexey Kurakin, Ian Goodfellow, and Samy Bengio. Adversarial examples in the physical world. *International Conference on Learning Representations Workshop*, 2017. 8
- [22] Alexey Kurakin, Ian J. Goodfellow, and Samy Bengio. Adversarial machine learning at scale. In *5th International Conference on Learning Representations, ICLR 2017, Toulon, France, April 24-26, 2017, Conference Track Proceedings*, 2017. 8
- [23] Yann LeCun, Léon Bottou, Yoshua Bengio, Patrick Haffner, et al. Gradient-based learning applied to document recognition. *Proceedings of the IEEE*, 86(11):2278–2324, 1998. 4
- [24] Xin Li and Fuxin Li. Adversarial examples detection in deep networks with convolutional filter statistics. In *IEEE International Conference on Computer Vision, ICCV 2017, Venice, Italy, October 22-29, 2017*, pages 5775–5783, 2017. 1, 8
- [25] Shih-Chieh Lin, Yunqi Zhang, Chang-Hong Hsu, Matt Skach, Md E Haque, Lingjia Tang, and Jason Mars. The architectural implications of autonomous driving: Constraints and acceleration. In *ACM SIGPLAN Notices*, volume 53, pages 751–766. ACM, 2018. 1
- [26] Aleksander Madry, Aleksandar Makelov, Ludwig Schmidt, Dimitris Tsipras, and Adrian Vladu. Towards deep learning models resistant to adversarial attacks. In *International Conference on Learning Representations*, 2018. 1, 4, 7, 8
- [27] Dongyu Meng and Hao Chen. Magnet: A two-pronged defense against adversarial examples. In *Proceedings of the*

- 2017 ACM SIGSAC Conference on Computer and Communications Security, CCS 2017, Dallas, TX, USA, October 30 - November 03, 2017, pages 135–147, 2017. 1, 8
- [28] Jan Hendrik Metzen, Tim Genewein, Volker Fischer, and Bastian Bischoff. On detecting adversarial perturbations. In *5th International Conference on Learning Representations, ICLR 2017, Toulon, France, April 24-26, 2017, Conference Track Proceedings*, 2017. 1, 8
- [29] Richard Meyes, Hasan Tercan, Simon Roggendorf, Thomas Thiele, Christian Büscher, Markus Obdenbusch, Christian Brecher, Sabina Jeschke, and Tobias Meisen. Motion planning for industrial robots using reinforcement learning. *Procedia CIRP*, 63:107–112, 2017. 1
- [30] Seyed-Mohsen Moosavi-Dezfooli, Alhussein Fawzi, and Pascal Frossard. Deepfool: a simple and accurate method to fool deep neural networks. In *Proceedings of the IEEE conference on computer vision and pattern recognition*, pages 2574–2582, 2016. 2, 3, 4, 8
- [31] Nicolas Papernot, Patrick McDaniel, and Ian Goodfellow. Transferability in machine learning: from phenomena to black-box attacks using adversarial samples. *arXiv preprint arXiv:1605.07277*, 2016. 8
- [32] Nicolas Papernot, Patrick McDaniel, Ian Goodfellow, Somesh Jha, Z Berkay Celik, and Ananthram Swami. Practical black-box attacks against machine learning. In *Proceedings of the 2017 ACM on Asia conference on computer and communications security*, pages 506–519. ACM, 2017. 8
- [33] Nicolas Papernot, Patrick D. McDaniel, Xi Wu, Somesh Jha, and Ananthram Swami. Distillation as a defense to adversarial perturbations against deep neural networks. In *IEEE Symposium on Security and Privacy, SP 2016, San Jose, CA, USA, May 22-26, 2016*, pages 582–597, 2016. 8
- [34] Omkar M Parkhi, Andrea Vedaldi, Andrew Zisserman, et al. Deep face recognition. In *bmvc*, volume 1, page 6, 2015. 1
- [35] Jérôme Rony, Luiz G Hafemann, Luiz S Oliveira, Ismail Ben Ayed, Robert Sabourin, and Eric Granger. Decoupling direction and norm for efficient gradient-based l2 adversarial attacks and defenses. In *Proceedings of the IEEE Conference on Computer Vision and Pattern Recognition*, pages 4322–4330, 2019. 1, 2, 3, 4, 6, 7, 8
- [36] Pouya Samangouei, Maya Kabkab, and Rama Chellappa. Defense-gan: Protecting classifiers against adversarial attacks using generative models. In *6th International Conference on Learning Representations, ICLR 2018, Vancouver, BC, Canada, April 30 - May 3, 2018, Conference Track Proceedings*, 2018. 1, 8
- [37] Karen Simonyan and Andrew Zisserman. Very deep convolutional networks for large-scale image recognition. In *3rd International Conference on Learning Representations, ICLR 2015, San Diego, CA, USA, May 7-9, 2015, Conference Track Proceedings*, 2015. 4
- [38] Yang Song, Taesup Kim, Sebastian Nowozin, Stefano Ermon, and Nate Kushman. Pixeldefend: Leveraging generative models to understand and defend against adversarial examples. In *6th International Conference on Learning Representations, ICLR 2018, Vancouver, BC, Canada, April 30 - May 3, 2018, Conference Track Proceedings*, 2018. 1, 8
- [39] Jiawei Su, Danilo Vasconcellos Vargas, and Kouichi Sakurai. One pixel attack for fooling deep neural networks. *IEEE Transactions on Evolutionary Computation*, 2019. 8
- [40] Christian Szegedy, Vincent Vanhoucke, Sergey Ioffe, Jonathon Shlens, and Zbigniew Wojna. Rethinking the inception architecture for computer vision. In *2016 IEEE Conference on Computer Vision and Pattern Recognition, CVPR 2016, Las Vegas, NV, USA, June 27-30, 2016*, pages 2818–2826, 2016. 6
- [41] Christian Szegedy, Wojciech Zaremba, Ilya Sutskever, Joan Bruna, Dumitru Erhan, Ian Goodfellow, and Rob Fergus. Intriguing properties of neural networks, 2013. 1
- [42] Cihang Xie, Jianyu Wang, Zhishuai Zhang, Zhou Ren, and Alan L. Yuille. Mitigating adversarial effects through randomization. In *6th International Conference on Learning Representations, ICLR 2018, Vancouver, BC, Canada, April 30 - May 3, 2018, Conference Track Proceedings*, 2018. 1, 8
- [43] Chiliang Zhang, Zhimou Yang, and Zuochang Ye. Detecting adversarial perturbations with saliency, 2018. 1, 5